The Additive Bachelier model with an application to the oil option market in the Covid period

Roberto Baviera[‡] & Michele Domenico Massaria[‡]

April 29, 2025

(‡) Politecnico di Milano, Department of Mathematics, 32 p.zza L. da Vinci, Milano

(preliminary version)

Abstract

In April 2020, the Chicago Mercantile Exchange (CME) temporarily switched the pricing formula for West Texas Intermediate oil market (WTI) options from the Black model to the Bachelier model. In this context, we introduce an Additive Bachelier model that provides a simple closed-form solution and a good description of the implied volatility surface.

This new Additive model exhibits several notable mathematical and financial properties. It ensures the no-arbitrage condition, a critical requirement in highly volatile markets, while also enabling a parsimonious synthesis of the volatility surface. The model features only three parameters, each one with a clear financial interpretation: the volatility term structure, vol-of-vol, and a parameter for modelling skew.

The proposed model supports efficient pricing of path-dependent exotic options via Monte Carlo simulation, using a straightforward and computationally efficient approach. Its calibration process can follow a cascade calibration: first, it accurately replicates the term structures of forwards and At-The-Money volatilities observed in the market; second, it fits the smile of the volatility surface.

Overall this model provides a robust and parsimonious description of the oil option market during the exceptionally volatile first period of the Covid-19 pandemic.

Keywords: volatility surface, Bachelier model, Additive process, cascade calibration.

JEL Classification: C51, G13.

Address for correspondence:
Roberto Baviera
Department of Mathematics
Politecnico di Milano
32 p.zza Leonardo da Vinci
I-20133 Milano, Italy
Tel. +39-02-2399 4575
roberto.baviera@polimi.it

The Additive Bachelier model with an application to the oil option market in the Covid period

1 Introduction

In April 2020, the price of oil futures contracts became negative for the first time in history. For this reason, the Chicago Mercantile Exchange (CME) and the Intercontinental Exchange (ICE) changed their models for oil from the Black to the Bachelier model for a time window (CME 2020, ICE 2020). That period corresponds to months when the Covid-19 pandemic spread globally characterized by a highly turbulent oil market and in particular for its options due to uncertainties related to both demand and supply (Shaikh 2021).

In this paper, we propose a new model that describes in a simple and parsimonious way all most liquid futures and options in the crude oil market for a time horizon.

There exist not many models that, on the one hand, account for negative prices in oil futures and, on the other, grant a coherent description for the whole volatility surface. The Bachelier model (Bachelier 1900, Davis and Etheridge 2006) allows for negative futures prices and reproduces the term structure of At-The-Money (ATM) volatilities without any smile. The Bachelier model assumes that stock prices follow a normal distribution, a significant departure from later models like Black and Scholes (1973), which assumes a log-normal distribution. Bachelier's framework has regained relevance in modern financial contexts, particularly in markets where asset prices can take near-zero or negative values, such as interest rate derivatives and certain commodity futures. Among possible extensions, one relevant enhancement replaces standard Brownian motions with Additive processes on real values (Carr and Torricelli 2021). These processes, which incorporate jumps and heavy-tailed distributions, improve the model's flexibility, enabling to capture more accurately the real-world behaviour of asset prices, especially in volatile markets.

The proposed model extends the Bachelier model to a class of Additive processes maintaining simple tractability and a coherent description for the whole volatility surface. When modelling oil derivatives, several are the advantages with existing Lévy models (a detailed description can be found in excellent textbooks, e.g., Cont and Tankov 2003): the proposed description offers a very simple calibration –known as cascade calibration– and it is able to reproduce exactly both the term structure of futures and ATM volatility, and describes the whole volatility surface with two additional parameters.

The model presents other key characteristics: i) it grants a closed form solution for plain vanilla call/put options; ii) it provides a simple analytical expression for the Implied volatility both around the ATM and for large moneynesses, always satisfying the no-arbitrage condition; iii) it offers an elementary calibration scheme, that reproduces first the most liquid derivatives, considering then the less liquid ones; iv) it enables very fast simulation techniques for path-dependent exotics.

Several are the contributions of this paper. Let us briefly summarize the three most relevant ones. First, we introduce a new model in the Bachelier framework that is particularly easy to handle analytically. Second, we show that –thanks to a separability property of the Implied vol– it is possible to implement a cascade calibration, i.e. the model is calibrated first on the most liquid products (discount-factors, ATM forwards), then on the ATM options, concluding with the rest of the volatility surface. Finally, we have calibrated on the WTI oil market in the whole time-window when the CME has considered Bachelier as the reference model (some months during the Covid-19 pandemic, when the market was very volatile) obtaining excellent results.

The rest of the paper is organized as follows. In Section 2, we introduce the Additive Bachelier model and its main properties. In Section 3, we describe the calibration scheme, named cascade calibration. In Section 4, we present the dataset and the main calibration results on the WTI oil market. Finally, we state our conclusions in Section 5.

2 The model

In this Section, we present the proposed model with a detailed description of its several interesting properties. The model presents an elementary closed formula in the Fourier space for plain vanilla options (Lewis Formula) thanks to its explicit characteristic function. Moreover, the proposed model grants a simple description in terms of Implied volatility and admits a cascade calibration, i.e. a calibration first on the most liquid financial products and then on the less liquid ones, a key property of a model among practitioners (see, e.g., Brigo and Morini 2005).

Let us call F_s the forward valued at time s and expiry at time t.
We model the forward with

$$F_s = F_0 + f_s \quad \forall s \in [0, t] \ , \tag{1}$$

where $\{f_s\}_{s\geq 0}$ a martingale process within a class of Additive processes. We call this dynamics for the forward either a *linear Additive process* or an *Additive Bachelier process*, because it is a natural extension of the *Bachelier* model.

We model the forward (1) specifying the characteristic function for the process. The underlying process $\{f_t\}_{t\geq 0}$ has characteristic function exponent

$$\ln \phi_t(u) := \ln \mathbb{E}\left[e^{i\,u\,f_t}\right] = \psi\left(i\,u\,\eta\,\sigma_t\,\sqrt{t} + \frac{u^2}{2}\,\sigma_t^2\,t;\ k,\ \alpha\right) + i\,u\,\eta\,\sigma_t\,\sqrt{t} \ , \tag{2}$$

with $k \in \mathbb{R}^+$, $\eta \in \mathbb{R}$ and σ_t a positive continuous function of time s.t. i) $\sigma_t^2\,t$ is increasing in time and ii) $\sigma_t^2\,t$ goes to zero for $t \to 0$. We indicate with $\mathbf{p}$ the set of three model parameters: k, η and σ_t.[1]
The quantity $\alpha \in [0, 1)$ is a hyper-parameter; it selects the chosen model: e.g. $\alpha = 0$ is related to the VG model (Madan and Seneta 1990) while $\alpha = 1/2$ to the NIG (Barndorff-Nielsen 1997). The function $\psi(u; k, \alpha)$ is defined as

$$\psi(u; k, \alpha) := \begin{cases} \dfrac{1}{k}\dfrac{1-\alpha}{\alpha}\left\{1 - \left(1 + \dfrac{u\,k}{1-\alpha}\right)^{\alpha}\right\} & \text{if } \ 0 < \alpha < 1 \\ -\dfrac{1}{k}\ln\left(1 + u\,k\right) & \text{if } \ \alpha = 0 \end{cases} . \tag{3}$$

Let us anticipate that the characteristic function in (2) is analytic in the horizontal strip with $\Im(u) \in (-p_t^-, p_t^+)$ with $p_t^{\pm} > 0$.[2].

The Bachelier model falls within this class (as shown in Appendix A); in this case, f_t is modelled via a Brownian motion W_t. Let us consider the European call option with strike K and maturity t; let us call B_0 the discount factor between value date $t_0 = 0$ and maturity t. Within the Bachelier model, the price for the European call with *moneyness* $x := K - F_0$ is

$$C_b(x, t; \sigma_t^b) = B_0\,\mathbb{E}_0\left[F_t - K\right]^+ = B_0\,\sqrt{t}\,c_b\left(\frac{x}{\sqrt{t}}, \sigma_t^b\right) = B_0\,\sigma_t^b\,\sqrt{t}\,c_b\left(\frac{x}{\sigma_t^b\,\sqrt{t}}, 1\right) \ , \tag{4}$$

[1] The definition (2) explains the reason why, we require that the volatility function σ_t is strictly positive. The case $\sigma_t = 0$ for all t describes the trivial (and non financial) situation with the characteristic function identically equal to 1, i.e. the forward F_t identically equal to its initial value F_0.

[2] This result is proven in Proposition 2.10.

where σ_t^b is the Bachelier volatility and c_b is a normalized Bachelier call price

$$c_b(y,\sigma) := -y\,\Phi\left(-\frac{y}{\sigma}\right) + \sigma\,\varphi\left(-\frac{y}{\sigma}\right) \tag{5}$$

with $\varphi(\bullet)$ and $\Phi(\bullet)$, respectively, the pdf and the CDF of a standard normal rv. Main properties of this formula are summarized in Appendix A.

The following Proposition states that the forward (modelled via (1) and the characteristic function (2)) is an Additive process (Sato 1999).

Proposition 2.1. *The process* $\{f_t\}_{t\geq 0}$ *with characteristic function* (2) *is Additive and martingale*

Proof. See Appendix B. □

This is a main property of the proposed model, because –being Additive– it is possible to simulate this process with an algorithm as fast as the simple Bachelier model that requires the simulation of only Gaussian rvs (see, e.g., Azzone and Baviera 2023). Thus, any structured product with a generic payoff can be priced and managed as a Bachelier model with similar characteristics in terms of simplicity and speed.
Moreover, as shown in the next Section this model provides a simple closed formula for European options, that is a generalization of the Lewis (2001) formula (see, e.g., Lee 2004b).

2.1 European call price closed formula

Let us consider the European call option (strike K, maturity t, moneyness x and discount factor B_0); the proposed model allows for a very simple pricing formula.

Proposition 2.2. (Call option Lewis formula)
When option's underlying is described by (1) *and* $\{f_t\}_{t\geq 0}$ *is an Additive martingale process with characteristic function* (2)*, analytic in the horizontal strip* $(-p_t^-, p_t^+)$ *with* $p_t^{\pm} > 0$*, the call option can be written as*

$$C(x,t;\mathbf{p}) = B_0\mathbb{E}[f_t - x] = B_0\left(R_a + \frac{e^{-xa}}{2\pi}\int_{-\infty}^{\infty}\phi_t(\xi - ia)\frac{e^{-i\xi x}}{(i\xi + a)^2}\mathrm{d}\xi\right) \tag{6}$$

for any $a \in (-p_t^+, p_t^-)$ *and*

$$R_a = \begin{cases} -x & \text{if } a \in (-p_t^+, 0) \\ -\dfrac{x}{2} & \text{if } a = 0 \\ 0 & \text{if } a \in (0, p_t^-) \end{cases}$$

Proof. See Appendix B. □

This closed formula for the European call allows us to price plain vanilla options in a simple and fast way way thanks to its Fourier transform formulation. The Additive Bachelier model grants also another call option formula.

Proposition 2.3. (A second call option formula)
When option's underlying process is described by $\{f_t\}_{t\geq 0}$ *with characteristic function* (2)*, the call option is given by*

$$C(x,t;\mathbf{p}) = B_0\,\sigma_t\sqrt{t}\;\mathbb{E}\left[c_b\left(\frac{x}{\sigma_t\sqrt{t}} + \eta\,(G-1), \sqrt{G}\right)\right] \tag{7}$$

where G *is a positive rv with Laplace exponent* $\psi(u;k,\alpha)$*, defined in* (3).

Proof. See Appendix B. □

This alternative pricing formula looks rather similar to the one of the Bachelier model: the Bachelier formula (4) corresponds to the case when G is identically equal to 1, i.e. $\psi(u; k, \alpha) = -u$ that corresponds to the limiting case $k \to 0$. On the one hand, this formulation enables some important properties of the Implied volatility, as discussed in the next Section, and, on the other hand, it leads to a simple model calibration. The latter property – probably the most important characteristic of the Additive Bachelier model – is presented in Section 3.

2.2 Implied volatility and its properties

The Implied volatility (hereinafter Implied vol) is a common description of model option prices. The Implied vol is defined as the value of the volatility which, when entered in the Bachelier option pricing model (4), returns a value equal to the model price (6) of that option. Thus, the Implied vol $\mathscr{I}_t(x)$ depends on option's moneyness x and maturity t and it is obtained solving the Implied vol (IV) equation

$$C_b(x, t; \mathscr{I}_t(x)) = C(x, t; \mathbf{p}) \quad . \tag{8}$$

Proposition 2.4. (Existence and uniqueness of the Implied vol)
Given $\{f_t\}_{t\geq 0}$, $\forall t \in \mathbb{R}^+$ and $\forall x \in \mathbb{R}$, it exists a unique $\mathscr{I}_t(x) \in \mathbb{R}^+$ solution of the IV equation (8).

Proof. See Appendix B. □

In the literature, some authors consider the *moneyness degree*, the moneyness divided by the squared root of the time-to-maturity (ttm), showing that in some cases is a natural model description (Carr and Wu 2003, Medvedev and Scaillet 2006). For the Additive Bachelier, the Implied vol $\mathscr{I}_t(x)$, written in terms of the (normalized) *moneyness degree*

$$y := \frac{x}{\sigma_t \sqrt{t}} \ , \tag{9}$$

has a very simple expression, as stated in the following proposition.

Proposition 2.5. (Separability of the Implied vol)
The Implied vol $\mathscr{I}_t(x)$ is a separable function of y and t

$$\mathscr{I}_t(x) = \sigma_t \, I(y) \, , \tag{10}$$

where $I(y)$ is time independent and can be obtained solving the following equation

$$c_b\left(y, I(y)\right) = \mathbb{E}\left[c_b\left(y + \eta\,(G-1), \sqrt{G}\right)\right] \ . \tag{11}$$

Proof. See Appendix B. □

By abuse of language, whenever there is no ambiguity, we call also $I(y)$ Implied vol or volatility smile, since it describes the volatility smile of the Implied vol.
The unique Implied vol $I(y)$ can be obtained solving the very simple IV equation (11) and it presents several interesting properties. In particular: i) it is a very regular function, being $\mathscr{C}^2(\mathbb{R})$, ii) its symmetry is regulated by the parameter η and iii) its expression is known both for small and large (normalized) moneyness degrees. These properties are described in the following propositions.

Proposition 2.6. (Regularity of I)
For any $k \in \mathbb{R}^+$ and $\eta \in \mathbb{R}$, $I(y)$ is $\mathscr{C}^2(\mathbb{R})$.

Proof. See Appendix B. □

Remark. It is possible to observe that for k equal to zero, the unique solution of the IV equation (11) is $I(y) = 1\ \forall y \in \mathbb{R}$, corresponding to the Bachelier model with time dependent deterministic volatility.

Proposition 2.7. (Symmetry of I)
$I(y; \eta) = I(-y; -\eta)$.

Proof. See Appendix B. □

Corollary 2.8. (I even function of y)
I is an even function of y, iff $\eta = 0$.

Proof. See Appendix B. □

The above properties suggest a comment on the parsimony of the proposed model. Not only the Additive Bachelier has few parameters being able to model the volatility surface with only three parameters. They also describe three main distinct aspects of the surface. As we'll discuss in detail in Section 3, σ_t models the term structure of the ATM volatility, i.e. controls the level of the volatility surface. Proposition 2.7 and Corollary 2.8 state that η models the skew, controlling the symmetry of the volatility, and for $\eta = 0$ describes the surface with a perfectly symmetric smile around the ATM. Finally k models the vol-of-vol, i.e. the convexity of the surface, being the limit $k \to 0$ the classical Bachelier model with no smile.

Proposition 2.9. (Implied volatility I for small $|y|$, i.e. close to the ATM)
The Implied volatility I around the ATM is

$$I(y) = I_0 + I_0'\, y + \frac{1}{2} I_0''\, y^2 + o(y^2)$$

where

$$\begin{cases} I_0 &= \sqrt{2\pi}\ \ \mathbb{E}\left[c_b\left(\eta\,(G-1), \sqrt{G}\right)\right] \\ I_0' &= -\sqrt{\dfrac{\pi}{2}}\ \ \mathbb{E}\left[\operatorname{erf}\left(\dfrac{\eta}{\sqrt{2}}\,\dfrac{1-G}{\sqrt{G}}\right)\right] \\ I_0'' &= \sqrt{2\pi}\ \ \mathbb{E}\left[\dfrac{1}{\sqrt{G}}\,\varphi\left(\eta\,\dfrac{1-G}{\sqrt{G}}\right)\right] - \dfrac{1}{I_0}\ , \end{cases} \tag{12}$$

with I_0' an odd function in η.

Proof. See Appendix B. □

These results are extremely relevant for both ATM volatility and volatility skew.
The ATM vol, using Implied vol separability (10), is

$$\sigma_t^{ATM} := \mathscr{I}_t(x=0) = \sigma_t\, I(y=0) = \sigma_t\, I_0 \tag{13}$$

i.e. the ATM volatility is proportional to σ_t, with the proportionality coefficient equal to I_0 in (12) that depends only of η and k. Moreover, the quantity I_0 is strictly positive due to the Jensen inequality

$$I_0 = \sqrt{2\,\pi}\,\mathbb{E}\left[-(\eta\,(G-1) + \sqrt{G}g)\right]^+ > \sqrt{2\,\pi}\,\left[\mathbb{E}(-\eta\,(G-1) - \sqrt{G}g)\right]^+ = 0\ .$$

This fact will play a key role in the model calibration scheme, as discussed in Section 3.

The volatility skew (often simply named skew) is defined as (see, e.g., Gatheral (2011))

$$skew := \left.\frac{\partial \mathscr{I}_t(x)}{\partial x}\right|_{x=0} .$$

It is proportional to I'_0. In fact, the skew is equal to

$$\left.\frac{\partial \mathscr{I}_t(x)}{\partial x}\right|_{x=0} = \sigma_t \left.\frac{\partial I(y)}{\partial y}\right|_{y=0} \frac{\partial y}{\partial x} = \frac{1}{\sqrt{t}} I'_0 . \tag{14}$$

The following result extends Lee (2004a) formula, providing the characterisation of the asymptotic behaviour of the Implied vol in the Additive Bachelier model.

Proposition 2.10. (Implied volatility I for large $|y|$)
The asymptotic behaviour of $I(y)$ for large y is

$$\lim_{y\to\pm\infty} \frac{I(y)^2}{|y|} = \frac{1}{2\,p^{\mp}}$$

with

$$p^{\pm} = \mp\eta + \sqrt{\eta^2 + 2\,\frac{1-\alpha}{k}} .$$

Proof. See Appendix B. □

3 Calibration scheme

Model parameters have a clear financial interpretation and – as already anticipated in the Introduction – they can be calibrated following a cascade calibration, i.e. a calibration procedure that includes the derivatives in several stages according to their liquidity.
The cascade calibration in option markets is the procedure desired by any market maker when calibrating a model. He/she would like to: first, reproduce the most liquid products (discount-rates and forwards/futures), then calibrate the most liquid options (ATM calls/puts) and finally fit the volatility surface for options that are either In-The-Money (ITM) or Out-The-Money (OTM). The idea is to get a more precise description of derivative contracts that are very liquid, thus present a narrow bid-ask spread as futures or ATM options, leaving only at a final stage the model calibration of the other options in the volatility surface, where trades are more rare and with larger bid-ask spreads.
The Additive Bachelier enables us to consider a model calibration in three stages: i) first, discount-rates and ATM forwards; ii) then, ATM options and iii) finally, all remaining traded options. As we'll show in the next Section such a calibration scheme is crucial in a very volatile market as the oil derivative market during the first Covid months.

First, the model can be calibrated exactly to the ATM forwards from market data. In particular, we follow the approach in Azzone and Baviera (2021), that allows us to extract from option prices precisely the term-structure used by option market makers of both (synthetic) forwards and discount-rates.

Second, we compute from option prices the term-structure of the ATM vol σ_t^{ATM}. We select the parameter σ_t proportional to the observed ATM vol σ_t^{ATM}. This calibration allows to reproduce exactly market ATM prices, in particular if we select the proportionality constant equal to I_0, as show in (13).

Finally, we desire to calibrate the last two parameters of the Additive Bachelier (η e k) on the volatility surface. We compute a *normalized moneyness* χ for the quoted options using the observed ATM forwards, ATM vol, maturities and strikes

$$\chi := \frac{x}{\sigma_t^{ATM}\sqrt{t}} \quad . \tag{15}$$

This quantity is equivalent to the moneyness degree (9), but differs for the constant I_0, having that two relations hold

$$\begin{cases} \sigma_t^{ATM} & = & I_0\,\sigma_t \\ y & = & I_0\,\chi \end{cases} \quad .$$

We have already discussed about the separability property (16) of the Implied vol, that enables to separate the dependence due to the term-structure (controlled by the parameter σ_t) and the one deriving from the moneyness. A similar property can be rewritten in terms of t and χ.

The Implied vol, for any option with maturity t, can be indicated in terms of χ as

$$\mathscr{I}_t(x) = \sigma_t^{ATM}\,\mathcal{I}(\chi) \tag{16}$$

where

$$\mathcal{I}(\chi) := \frac{I(\chi\,I_0)}{I_0}$$

does not depend from the maturity t, as stated in the following proposition.

Proposition 3.1. *Model IV equation* (11) *is equivalent to*

$$c_b\left(\chi, \mathcal{I}(\chi)\right) = \mathcal{C}(\chi; \eta, k)\ , \tag{17}$$

where

$$\mathcal{C}(\chi; \eta, k) := \frac{1}{I_0}\mathbb{E}\left[c_b\left(\chi\,I_0 + \eta\,(G-1), \sqrt{G}\right)\right] \quad ,$$

and the Implied vol $\mathcal{I}(\chi)$*, unique solution of* (17)*, does not depend on* t*.*

Proof. See Appendix B. □

Let us observe that the right hand side of the IV equation (17), $\mathcal{C}(\chi; \eta, k)$, depends only on the parameters η, k. Thus, $\mathcal{I}(\chi)$ is function of only this two parameters, while it does not depend on σ_t. This separability property is important and allows us to separate the calibration in three stages.

1. Calibrate ATM forwards and discount-rates on market data;
2. Identify σ_t^{ATM} on quoted options and choose σ_t equal to σ_t^{ATM}/I_0 for every maturity t;
3. Calibrate the two parameters η, k on OTM option prices normalized by σ_t^{ATM}.

As already mentioned, the first two stages are able to reproduce exactly both the term structures of forwards and ATM vol. The last stage leverages on the properties of the Implied vol surface (in particularly the separability (16) of the Implied vol discussed above) and requires some more comments. Once the σ_t^{ATM} has been identified, one has to i) compute the χ_i –the *moneyness* normalized by ATM vol as in (15)– for all quoted options, ii) compute for each option $\mathcal{C}^{mkt}(\chi_i)$, the price normalized by B_0, $\sqrt{t}$ and σ_t^{ATM} for all quoted options and iii) minimize the L^2-distance between the quoted market prices $\mathcal{C}^{mkt}(\chi_i)$ and the corresponding model prices $\mathcal{C}(\chi_i; \eta, k)$

$$d(\eta, k) := \sum_i \left[\mathcal{C}^{mkt}(\chi_i) - \mathcal{C}(\chi_i; \eta, k)\right]^2 \ ,$$

selecting the optimal values of η and k.[3]
Finally, the normalized Implied vol is $\mathcal{I}(\chi)$ can be obtained via the Implied vol equation (17). The calibrated Implied vol is

$$\mathscr{I}_t\left(x\right) = \sigma_t^{ATM} \, \mathcal{I}\left(\frac{x}{\sigma_t^{ATM}\sqrt{t}}\right) \ .$$

We observe that this calibration method reproduces exactly market ATM volatility. In fact, ATM $\mathcal{C}(0; \eta, k)$ is equal to $(2\,\pi)^{-1/2}$ for every η and k, thus $\mathcal{I}\left(0\right) = 1$.

A property that describes well the Implied vol surface in some markets (e.g. the equity and interest rate markets) is *sticky delta*. Sticky delta describes the situation where the Implied volatility, when the underlying moves, remains unchanged (i.e., it sticks) with the moneyness.

Lemma 3.2. (Stickiness of the Implied vol)
Additive Bachelier Implied vol is sticky delta.

Proof. The proposed model is naturally sticky delta, i.e. keeping constant the model parameters $\mathbf{p}$, the whole volatility surface as a function of the moneyness does not change. □

This model property is a great advantage from practitioners' perspective: hedges derived from this model remain stable if the market moves according to the sticky delta rule.
In the next Section, we'll observe that while the model fits exactly the most liquid products (discount-rate, forward and ATM vol), the other parameters (η and k) remain relatively constant even in the high-volatile oil market of the first Covid months.[4]

4 Calibration results

In this Section, we present the results of the calibration on market data of the proposed model, comparing the results with three natural benchmarks.

In Section 4.1, we describe the data used in the analysis; in Sections 4.2 and 4.3, we show the results of the calibration. In particular in Section 4.2, we show the results for all the value dates considered in this analysis. In Section 4.3, we focus on a value date in the dataset, the 29$^{\text{th}}$ of April 2020 (one week after the announce from CME (2020)), comparing our results with market data and the three benchmark models.

[3]The model is calibrated on both calls and puts, considering the OTM options.

[4]A trader that keeps hedged his/her portfolio, in practice hedges exposures generated (according to a given model) by model parameters that –ideally– correspond to different risks (e.g. underling, discount-rate, ATM vol, skew, etc...). If these parameter remain relatively constant over time when market conditions do not change significantly he/she avoids to pay transaction costs on trades due to exposures generated by an inadequate model description.

4.1 Dataset

The dataset is composed by daily market prices of call and put options on the West Texas Intermediate (WTI) oil futures traded on the Chicago Mercantile Exchange (CME). We consider the whole period when the CME has switched the options pricing and valuation model to Bachelier (CME 2020). The time-window of interest goes from the 23$^{\text{rd}}$ of April 2020 to the 31$^{\text{st}}$ of August 2020. Data are present in all weekdays with the exception of two public holidays in the USA: the 25$^{\text{th}}$ of May 2020 (Memorial Day) and the 3$^{\text{rd}}$ of July 2020 (Independence Day Holiday), where no options were traded. Daily prices are obtained from Bloomberg. The options are quoted for a grid of strikes that goes from 2.5 \$ to 245 \$. The grid size is equal to 0.5 \$ from 5 \$ to 146.5 \$, it's equal to 2.5 \$ from 147.5 \$ to 195 \$, and it's 5 \$ from 195 \$ to 245 \$. We consider all available liquid options' expiry: from June 2020 (JUN20) to December 2022 (DEC22). We have considered as "risk-free" rate the Effective Federal Funds Rate OIS curve in the time-window of interest up to the three years expiry. In Table 1, we report a summary statistics.

	Min	Max	#
Value Dates	23$^{\text{rd}}$ of April 2020	31$^{\text{st}}$ of August 2020	93
Strikes	2.5 \$	245 \$	314
Expiries	JUN20	DEC22	9

Table 1: Value dates, grid of strikes and option expiries in the dataset. We report the number of value dates, strikes and expiries in the dataset.

From this dataset, we first replicate discount-rates and ATM forwards from option prices, as described in Azzone and Baviera (2021). To do so, we need the couples of call and put options traded for the same strike and expiry, for each value date. In Table 2, we show the number of couples of options available for each value date in the period of the analysis, we report mean, median, standard deviation (std), and quantiles (q) 5%, 95%.

	JUN20	SEP20	DEC20	MAR21	JUN21	SEP21	DEC21	JUN22	DEC22
Mean	148	104	100	19	22	4	24	3	7
Median	148	107	114	18	21	4	24	3	8
Std	0	17	30	7	5	2	5	1	2
$q_{0.05}$	148	96	28	11	17	1	16	0	4
$q_{0.95}$	148	114	117	31	30	6	29	3	9

Table 2: We report the number of call-put options' couples traded for each maturity and value date: mean, median, standard deviation (std), and quantiles (q) 5%, 95% considering each value date.

After having taken into account the ATM vol, we desire to calibrate the two parameters of the Additive model from OTM options. We consider OTM call options ($K > F_0$) and OTM put options ($K < F_0$) in the range of moneyness $x \in [-30\,\$, 30\,\$]$.
In Table 3, we provide the descriptive statistics of the number of available OTM options, for all the strikes and value dates, we report mean, median, standard deviation (std), and quantiles (q) 5%, 95%.

# OTM opt.	JUN20	SEP20	DEC20	MAR21	JUN21	SEP21	DEC21	JUN22	DEC22
Mean	92	116	105	58	49	13	49	10	24
Median	92	120	119	51	46	13	54	9	26
Std	9	7	27	25	7	3	9	1	6
$q_{0.05}$	76	101	30	26	42	7	26	8	7
$q_{0.95}$	103	120	120	94	63	17	56	11	28

Table 3: Number of OTM options considered in the Volatility surface calibration. We report the number of OTM call ($K > F_0$) and put ($K < F_0$) in the moneyness range $[-30\,\$, 30\,\$]$: mean, median, standard deviation (std), and quantiles (q) 5%, 95% considering each value date.

We observe from these tables that the market in the period of interest (from April 2020 to August 2020) was relatively illiquid. We'll notice in the following that, despite these market conditions, our model is able to describe adequately the key features of this market, with stable results across the value dates in the period of interest.

4.2 A glimpse on all value dates

In this Section, we present the results for all value dates in the dataset; in particular, we show the spread of options' discount-rates on the OIS rates, and the parameters η and k of the Additive model; we present their evolution across the different value dates.

Figure 1 shows the spread of the discount-rates derived from option prices on the "risk-free" rates (OIS) for different value dates. In blue line (dots and continuous line, left axis), we can see the spread corresponding to the first maturity: this quantity shows a rapid increase when approaching the first expiry. The average of the corresponding spread on all the other expiries is plotted in green (squares and dashed line, right axis). We observe that the latter remains of the order of few basis points (on average around 2 bps), i.e. negligible for all practical purposes in the volatile market of the first Covid period, and it is much smaller than the spread on the first expiry (even of 2 orders of magnitude), that reaches some hundreds of basis points. The inability to reproduce even OIS rates is a clear indicator of market distress. The observed behaviour of option discount-rates for very short-term maturities highlights the extremely tough market conditions that the WTI oil market experienced during the Covid period.

For this reason, the options on the first expiry are not considered in the calibration procedure when the discount-rates are significantly different from the "risk-free" rates; in particular, the adopted criteria is to consider the first expiry when the spread is up to one order of magnitude larger than the average spread (i.e. it is less than 20 bps).

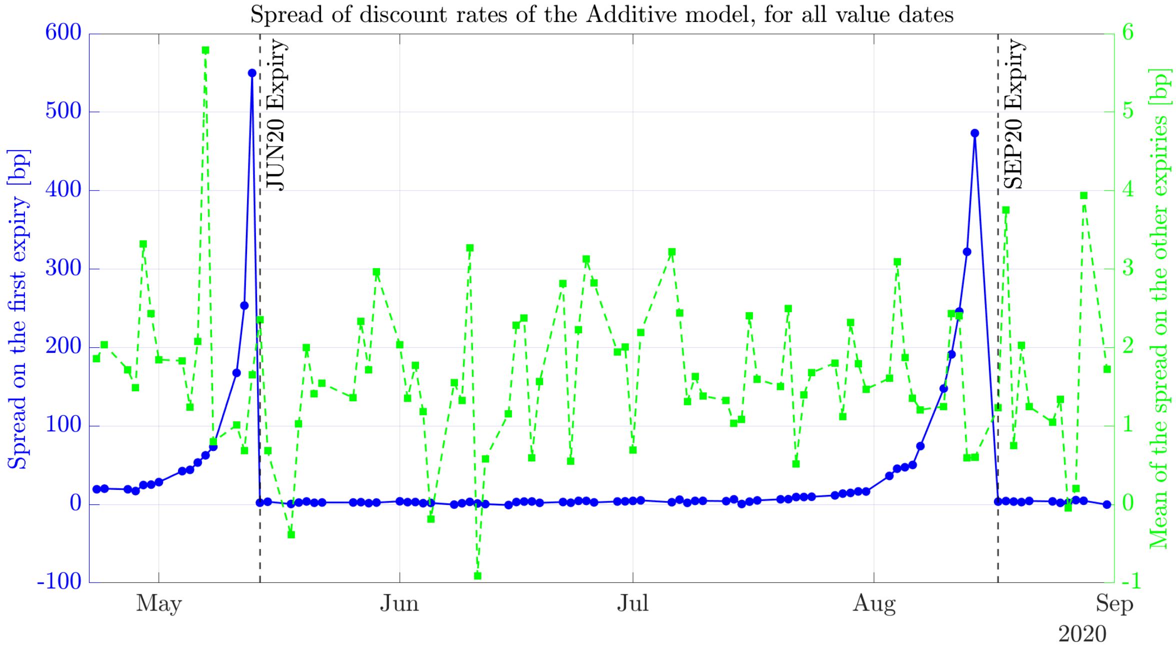

Figure 1: Spread of the discount-rates (from option prices) on the OIS curve, for all value dates considered in the analysis. The vertical lines correspond to the expiries of the first two options. In blue (dots and continuous line, left axis), we can see the spread corresponding to the first maturity: we observe that it rapidly increases when approaching options' first expiry, reaching some hundreds of basis points. In green (squares and dashed line, right axis), we see the average of the spread corresponding to the other expiries: we can observe that it is of few basis points (an average 2 bps), i.e. its order of magnitude is much smaller than the spread for the first expiry.

Following the cascade calibration described in Section 3, we calibrate the parameter η and k of the Additive model, for the different value dates, with the choice of $\alpha = 1/2$ (the results for other values of α are similar). In Figures 2 and 3, we show these two parameters for all value dates.

In Figure 2, we show the values of the parameter η over the period of interest. This parameter moves in time, but slowly and exhibiting no significant oscillations.

Figure 3 shows the behaviour of the parameter k for the different value dates during the analysed period. After a rapid increase in the last days of April (the week after the announce from CME (2020)), that reflects an initial market adjustment, this parameter remains close to one in the period of the analysis, moving slowly over time.

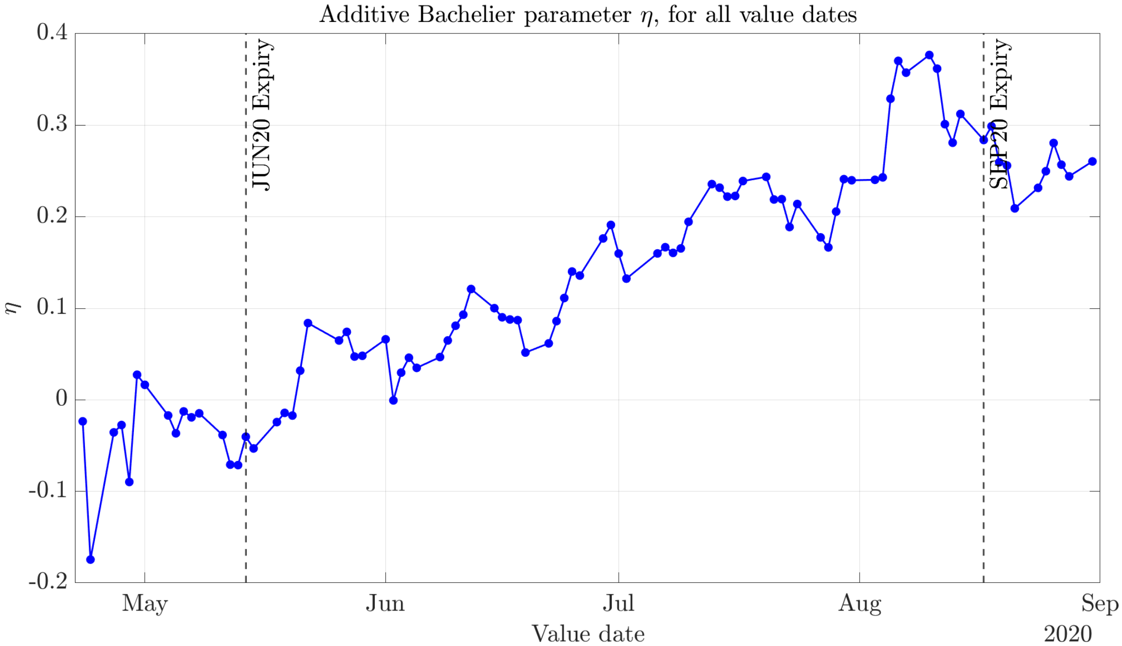

Figure 2: Parameter η of the Additive Bachelier calibrated for the different value dates considered in the analysis. The vertical lines correspond to the expiries of the first two options. We observe that its value does change significantly for the value dates but it moves slowly over time.

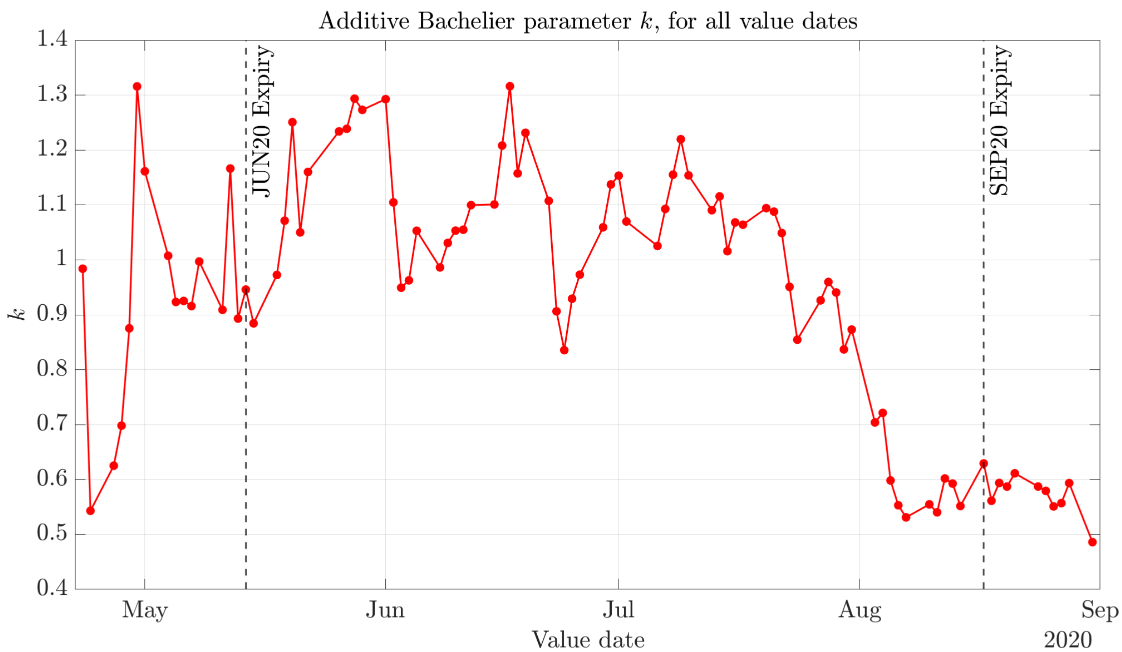

Figure 3: Parameter k of the Additive Bachelier calibrated for the different value dates considered in the analysis. The vertical lines correspond to the expiries of the first two options. We observe that its value is rather close to one and moves slowly over time.

As already mentioned commenting Tables 2 and 3, the WTI derivative market was not relatively illiquid in the time-window of interest. We highlight that, despite the observed high volatility and low liquidity market, it is possible to achieve stable results over time in the calibration the Additive Bachelier parameters (η and k). In the following Section, let us discuss the calibration results achieved on a single value date.

4.3 Detailed results for one date: the 29$^{\text{th}}$ of April 2020

In this Section, we show the results with value date on the 29$^{\text{th}}$ of April 2020 (one week after the announce from CME (2020), in one of the most volatile periods),[5] compared with the results of other three models considered as benchmarks:

- the Lévy model, defined in (20),
- a Lévy model that includes options with one ttm at time (Lévy fixed ttm),
- an Additive Logistic model (see Carr and Torricelli 2021).

The first benchmark is the simplest generalization of Bachelier model that allows for a volatility surface, while the second is the same model but calibrated considering separately the options with a given ttm: the latter utilizes a different set of parameters for each maturity and it is not in general a coherent model for the whole volatility surface but –as we'll show in this Section– it reproduces quite accurately the market volatility surface. The last one is an example of Additive processes applied to real-valued underlying.

In Figure 4, we compare the discount-rates (from option prices) with the "risk-free" rates from the Effective Federal Funds Rate OIS curve. We see that the spread on the first expiry is larger than 20 basis points, while the spread corresponding to the other expiries is much smaller.

As already mentioned, since the spread on the first date is larger than 20 basis points, we do not consider the first expiry in the next steps of the calibration.

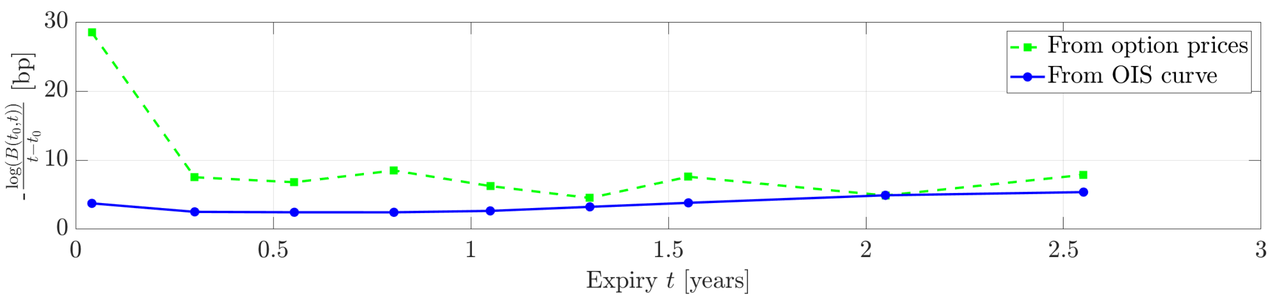

Figure 4: Discount-rates from option prices (in green, squares and dashed line), and the "risk-free" rates from the OIS curve (in blue, dots and continuous line) observed in the market on the 29$^{\text{th}}$ of April 2020.

After replicating discount-rates and ATM forward, we consider the ATM volatility.

In Figure 5, we plot the ATM volatility from market Implied volatility with the ATM volatility from the calibration of the Lévy model (black dashed line in Figure 5), the Additive Logistic (cyan continuous line in Figure 5), the Lévy fixed ttm (green dot-dashed lines) and the Additive Bachelier model (blue dot and continuous line). The Lévy fixed ttm and the Additive Bachelier model reproduce exactly the ATM volatility term structure, while both the Lévy model and the Additive Logistic are not able to replicate the ATM volatility term structure.

[5] Results do not appear significantly different on all other value dates and they are available upon request.

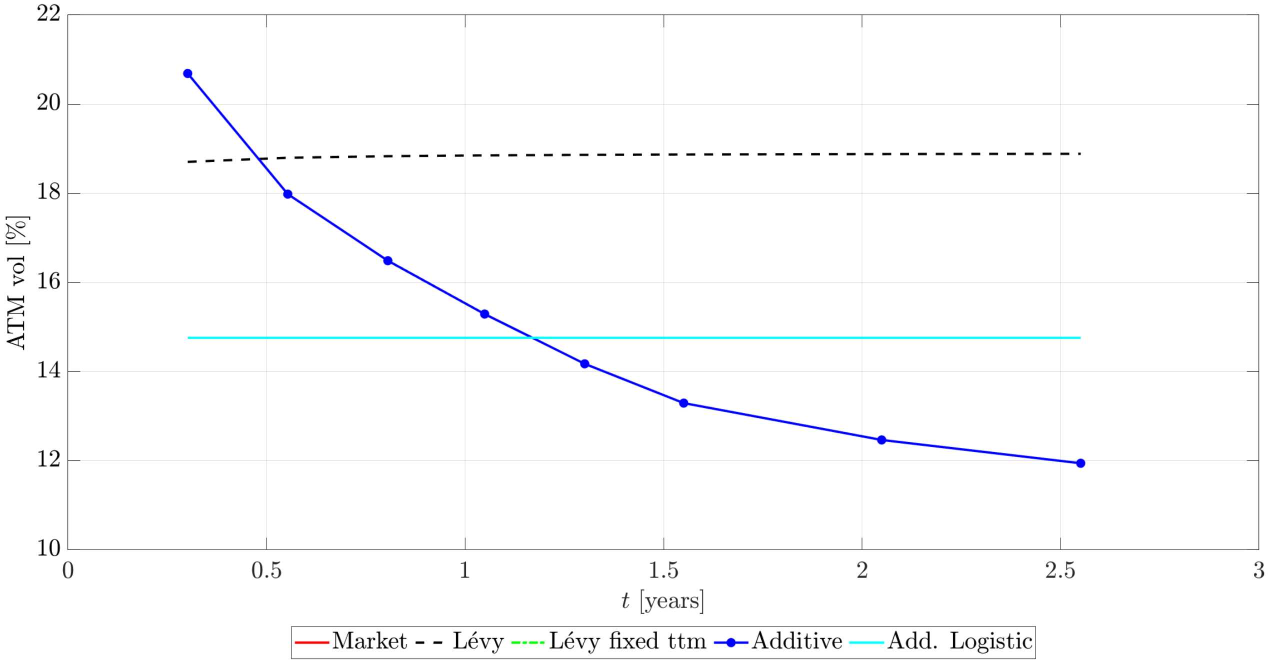

Figure 5: ATM volatility comparison between market data (red, continuous line), the Additive model (in blue, dots and continuous line), the Lévy fixed ttm (green, dots dashed line), the Lévy model (black, dashed line) and the Additive Logistic (cyan, continuous line), on the 29^{th} of April 2020, for $\alpha = 1/2$. While the first three are indistinguishable in the figure with both the Lévy fixed ttm and the Additive Bachelier replicating exactly market ATM vol, both the Lévy model and the Additive Logistic are not able to reproduce the ATM vol.

Then we can calibrate the Implied volatility surface for the models discussed. In Figure 6, we plot the volatility smile for all option maturities (without considering the first one), with value date the 29^{th} of April 2020. We consider all options with moneyness x in the range $[-30\,\$, 30\,\$]$. We show the results of the Lévy Bachelier (black dashed lines), the Lévy fixed ttm (green dot-dashed lines), the Additive Logistic (cyan continuous lines) and the Additive Bachelier (blue dots), considering $\alpha = 1/2$. We observe that results from the Lévy model and the Additive Logistic model cannot be considered adequate, since they fail to be replicate the volatility smile in all the eight expiries. The calibration provided by "Lévy fixed ttm" replicates accurately market data. Finally, the Additive Bachelier provides a quite good calibration of the Implied volatility surface over all considered expiries despite its parsimony.

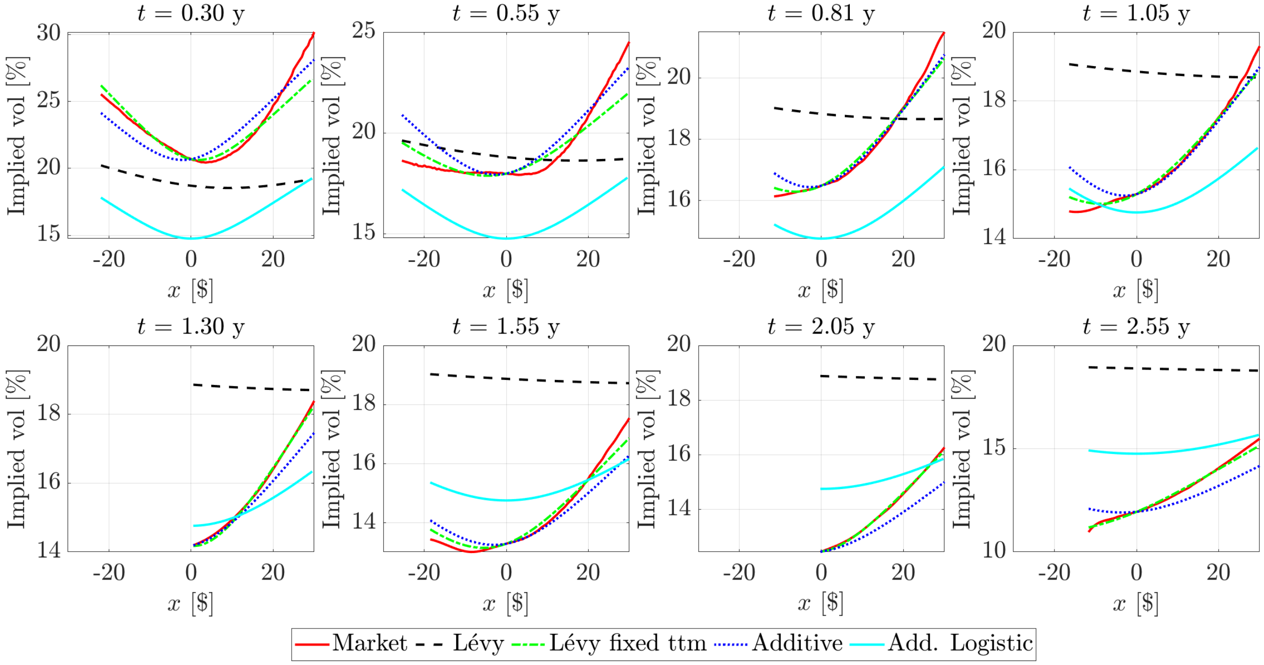

Figure 6: Volatility surface. We plot the volatility smile for each option maturity present in the dataset after the first one, for the value date 29$^{\text{th}}$ of April 2020. We consider all options with moneyness x in the interval $[-30\,\$, 30\,\$]$, for some maturities this moneyness interval is even larger than the observed market prices. Market Implied vol (red continuous lines) is plotted together with the three models discussed in the text: the Lévy Bachelier (black dashed lines), the Lévy that includes options with one ttm at time (Lévy fixed ttm, green dot-dashed lines), the Additive Logistic model (cyan, continuous lines) and the Additive Bachelier (blue dots). While results for the Lévy and Additive Logistic model cannot be considered adequate, the calibration provided by Lévy fixed ttm replicates accurately market data and the Additive Bachelier provides values quite close to the latter. We consider $\alpha = 1/2$.

We compare the results for the three model observing the mean squared error (MSE) of model prices wrt market prices divided for each maturity t (with moneyness in the interval $[-30\,\$, 30\,\$]$). We plot in Figure 7 the MSE from each model for all the expiries (except for the first one) present in the dataset.

We observe that the error from the Lévy model and the Additive Logistic are almost two orders of magnitude (three for longer expiries in the case of the Lévy model) larger than the MSE of the Lévy fixed ttm, and at least one order of magnitude larger that the error of the Additive Bachelier (in blue, dots and continuous line), that is quite close to the one of the Lévy fixed ttm for expiries up to one year, becoming larger for longer expiries.

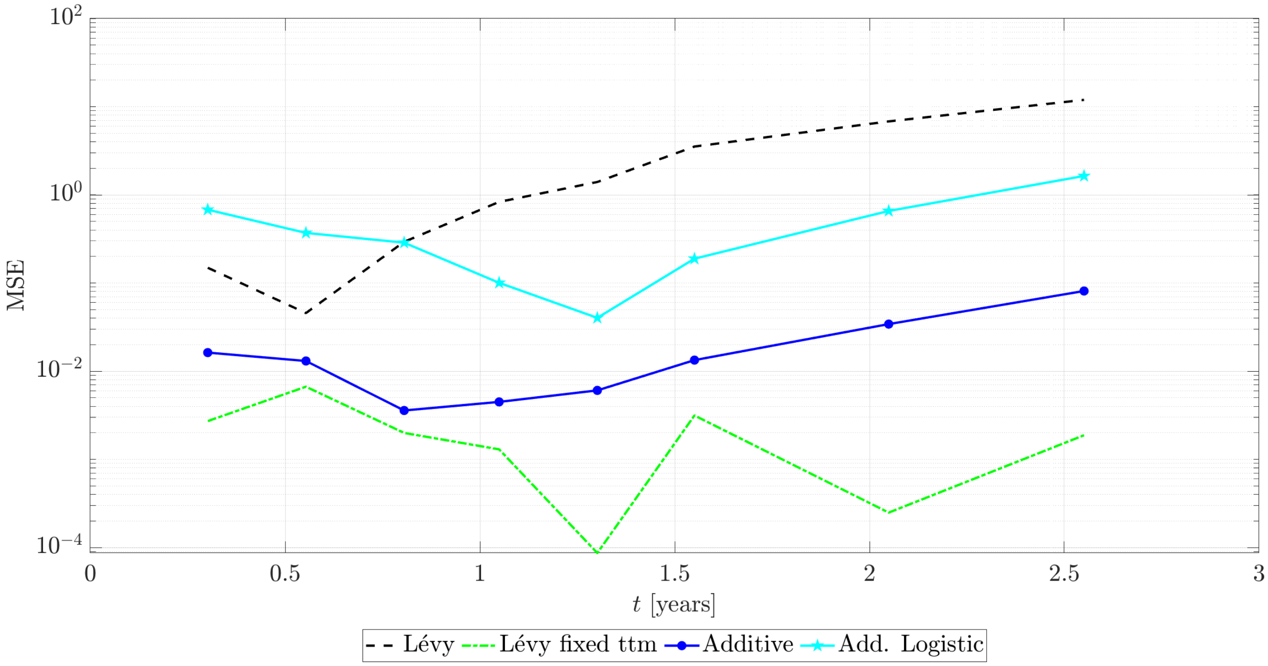

Figure 7: Comparison of the MSE obtained when calibrating the Lévy model (in black, dashed line), the Lévy fixed ttm (green, dots dashed line), the Additive Logistic model (cyan, stars and continuous line) and the Additive Bachelier (blue, dots and continuous line) in the 29$^{\text{th}}$ of April 2020, for $\alpha = 1/2$. The Lévy model and the Additive Logistic present an MSE almost two orders of magnitude larger than Lévy fixed ttm, while MSE for Additive Bachelier is rather close (expecially for options with maturity up to 1 year) to the Lévy fixed ttm.

Figure 8 shows the calibrated parameters η and k of the Additive Bachelier (blue, continuous, constant lines). The green squares (with dashed lines) correspond to the parameters of the Lévy fixed ttm, for all the expiries. The close alignment between the two kind of parameters suggests that the Additive Bachelier parameters exhibit consistency across maturities.

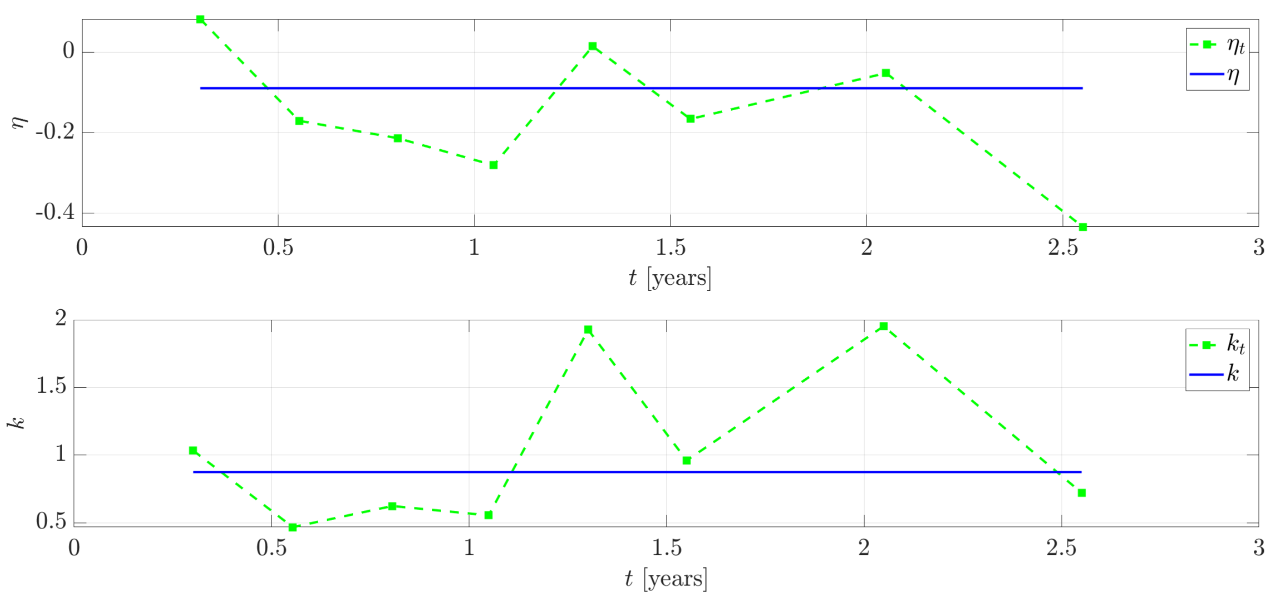

Figure 8: Parameters η, k of the Additive Bachelier (blue continuous line), compared with the parameters η_t, k_t of the Lévy fixed ttm. They appear quite similar for all options after the first expiry traded in the market. The top panel shows the parameter η, and the bottom panel shows the parameter k.

5 Conclusions

This paper has introduced the Additive Bachelier, an extension of the Bachelier framework, to describe the WTI oil options.

The proposed model allows for negative prices and it is very simple from an analytical point of view, allowing for explicit expression of the Implied vol close to ATM and for very large moneyness. Key features of the model include:

- A closed-form solution for European options pricing, based on the Lewis formula.
- A cascade calibration approach that prioritizes the most liquid instruments, ensuring consistency in the pricing of ATM forward prices, ATM volatilities, and the Implied volatility surface.
- The ability to synthesize the entire volatility surface using just two parameters, each of them with a clear financial interpretation, facilitating practical application.

The calibration results (discussed in Section 4) highlight the robustness of the proposed model over a very volatile period as the first period of the Covid-19 pandemic, ensuring a stable calibration for different value dates in the period from April 2020 to August 2020, and reproducing quite closely key market features.

Appendix A: Bachelier formula, Lévy Bachelier and its generalization

Bachelier formula basic properties

We briefly recall some basic properties of the normalized Bachelier formula $c_b(y,\sigma)$ defined in (5). It can be obtained as

$$c_b(y,\sigma) = \mathbb{E}[-\sigma g - y]^+$$

with g a standard normal rv.
It is a positive homogeneous function (of degree one)

$$c_b(\lambda\, y, \lambda\, \sigma) = \lambda\, c_b(y,\sigma) \quad \forall \lambda > 0 \ . \tag{18}$$

The time-value defined as the difference between price and payoff is

$$TV(y,\sigma) = -|y|\, \Phi\left(-\frac{|y|}{\sigma}\right) + \sigma\, \varphi\left(-\frac{|y|}{\sigma}\right)$$

is symmetric w.r.t the moneyness-degree.

Bachelier Greeks

$$\begin{array}{llcll}
\text{Delta} & \Delta_b & := & \dfrac{\partial}{\partial(-y)} c_b(y,\sigma) & = \Phi\left(-\dfrac{y}{\sigma}\right) \ , \\
\text{Vega} & \mathscr{V}_b & := & \dfrac{\partial}{\partial \sigma} c_b(y,\sigma) & = \varphi\left(-\dfrac{y}{\sigma}\right) \ , \\
\text{Gamma} & \Gamma_b & := & \dfrac{\partial^2}{\partial(-y)^2} c_b(y,\sigma) & = \dfrac{1}{\sigma}\varphi\left(-\dfrac{y}{\sigma}\right) \ , \\
\text{Vanna} & vanna_b & := & \dfrac{\partial}{\partial(-y)}\dfrac{\partial}{\partial \sigma} c_b(y,\sigma) & = \dfrac{y}{\sigma^2}\varphi\left(-\dfrac{y}{\sigma}\right) \ .
\end{array} \tag{19}$$

Lévy Bachelier model

The Bachelier model is not able to describe any volatility surface. The simplest generalization is a Bachelier Lévy model defined through its Normal Tempered Stable characteristic function

$$\ln \phi_t(u) := \ln \mathbb{E}\left[e^{i\,u\,f_t}\right] = t\left(\psi\left(i\,u\,\hat{\eta}\,\hat{\sigma} + \frac{u^2}{2}\,\hat{\sigma}^2; \hat{k},\ \alpha\right) + i\,u\,\hat{\eta}\,\hat{\sigma}\right)\ , \tag{20}$$

with $\hat{\eta} \in \mathbb{R}$ and $\hat{\sigma}, \hat{k} \in \mathbb{R}^+$. This model is the generalization to the linear (Bachelier) case of the Normal Tempered Stable exponential Lévy model that can be found in excellent text books (see, e.g., Cont and Tankov 2003).
This model unfortunately is not able to reproduce adequately the observed volatility surface, as also shown in Section 4. However, a Lévy model that is calibrated on one single maturity at a time (called "Lévy fixed ttm" in the text) is able to calibrate in an excellent way even the oil derivative market in the most turbulent period that has been observed so far: the first months of the Covid pandemic. Clearly, this model has a set of parameters that vary at each maturity and the model is not necessarily well posed.
For this reason we would like to consider the natural inhomogeneous extension of the Lévy process case (20), where the parameters are time dependent, as described in the following Lemma.

Lemma A.1. (A class of Additive processes $\{f_t\}$)
Given the continuous deterministic functions of time σ_t strictly positive and such that $\sigma_t^2 t$ goes to zero for $t \to 0$, $\eta_t \in \mathbb{R}$ and $k_t \in \mathbb{R}^+$, and $\alpha \in [0, 1)$, the class of processes $\{f_t\}_{t\geq 0}$ with characteristic function exponent

$$\ln \phi_t(u) := \ln \mathbb{E}\left[e^{i\,u\,f_t}\right] = \psi\left(i\,u\,\eta_t\,\sigma_t\,\sqrt{t} + \frac{u^2}{2}\,\sigma_t^2\,t;\ k_t,\ \alpha\right) + i\,u\,\eta_t\,\sigma_t\,\sqrt{t}\ , \tag{21}$$

is Additive when the following conditions hold true:

1. *The functions*

$$\begin{aligned} p_t^{\pm} &:= \frac{1}{\sigma_t\sqrt{t}}\left\{\mp\eta_t + \sqrt{\eta_t^2 + 2\,\frac{1-\alpha}{k_t}}\right\} \\ p_t^{*} &:= -\frac{t^{1/2}\sigma_t}{k_t^{(1-\alpha)/\alpha}}\sqrt{\eta_t^2 + 2\,\frac{1-\alpha}{k_t}} \end{aligned}$$

   are non-increasing;

2. *$\sqrt{t}\,\sigma_t\,\eta_t$ and $\sqrt{t}\,\sigma_t\,\eta_t\,k_t^{(\alpha-1)/\alpha}$ go to zero as t goes to zero.*

Proof. At any given time $t > 0$, we have the expression for the generating triplet for a process with characteristic function exponent (21) (see, e.g., Cont and Tankov 2003, eq.(4.24), p.130)

$$\begin{cases} A_t &= 0 \\ \gamma_t &= \int_{|x|<1} x\,\nu_t(\mathrm{d}x) + \eta_t\sigma_t\sqrt{t} \\ \nu_t(x) &= \frac{C(\alpha,k_t,\sigma_t,\eta_t)}{|x|^{\alpha+1/2}}\,e^{-\frac{\eta_t\,x}{\sigma_t\sqrt{t}}}\,K_{\alpha+1/2}\left(|x|\frac{\sqrt{\eta_t^2+2\frac{1-\alpha}{k_t}}}{\sigma_t\sqrt{t}}\right) \end{cases}$$

where

$$C(\alpha, k_t, \sigma_t, \eta_t) = \frac{2}{\Gamma(1-\alpha)\sqrt{2\pi}\sigma_t\sqrt{t}}\left(\frac{1-\alpha}{k_t}\right)^{1-\alpha}\left(\sqrt{\eta_t^2\sigma_t^2 t + 2\sigma_t^2 t\frac{1-\alpha}{k_t}}\right)^{\alpha+1/2}\ ,$$

and

$$K_\theta(z) = \frac{e^{-z}}{\Gamma(\theta+1/2)}\sqrt{\frac{\pi}{2z}}\int_0^{+\infty} e^{-s}s^{\theta-1/2}\left(\frac{s}{2z}+1\right)^{\theta-1/2}\mathrm{d}s$$

is the modified Bessel function of the second kind (see, e.g., Abramowitz and Stegun 1948, Ch.9, p.376). For $t=0$, we set $A_0=0$, $\gamma_0=0$ and $\nu_0=0$.

First, we prove that $\nu_t(x)$ is not an increasing function wrt t. The expression for $\nu_t(x)$ is the following

$$\begin{aligned}\nu_t(x) =& \frac{(1-\alpha)^{1-\alpha}}{\Gamma(1-\alpha)\Gamma(1+\alpha)|x|^{\alpha+1}} \exp\left\{-\frac{1}{\sigma_t\sqrt{t}}\left(x\eta_t + |x|\sqrt{\eta_t^2+2\frac{1-\alpha}{k_t}}\right)\right\} \\ & \int_0^{+\infty} e^{-s}s^\alpha\left[\frac{\sigma_t^2 t}{k_t^{(1-\alpha)/\alpha}}\left(\frac{s}{2|x|}+\frac{1}{\sigma_t\sqrt{t}}\sqrt{\eta_t^2+2\frac{1-\alpha}{k_t}}\right)\right]^\alpha \mathrm{d}s\end{aligned}$$

The function $\nu_t(x)$ is not decreasing wrt t $\forall x$ if the following two terms are not decreasing

$$\exp\left\{-\frac{1}{\sigma_t\sqrt{t}}\left(x\eta_t + |x|\sqrt{\eta_t^2+2\frac{1-\alpha}{k_t}}\right)\right\} \tag{22}$$

$$\frac{\sigma_t^2 t}{k_t^{(1-\alpha)/\alpha}}\left(\frac{s}{2|x|}+\frac{1}{\sigma_t\sqrt{t}}\sqrt{\eta_t^2+2\frac{1-\alpha}{k_t}}\right) \; . \tag{23}$$

The condition on $p_t^\pm$ implies that (22) is not decreasing wrt t $\forall x \in \mathbb{R}$. The condition on $p_t^\pm$ implies also that

$$\frac{1}{\sigma_t\sqrt{t}}\sqrt{\eta_t^2+2\frac{1-\alpha}{k_t}}$$

is not increasing, thus the factor $\sigma_t^2\, t\, k_t^{(\alpha-1)/\alpha}$ is not decreasing and that also (23) is not decreasing.

To prove that

$$\lim_{t\to 0}\nu_t(x) = 0 \quad \forall x \neq 0 \tag{24}$$

we discuss three cases (whose union covers all possible cases)

$$\begin{aligned} &\text{a)} \quad \lim_{t\to0}\eta_t^2 k_t = 0 \; , \\ &\text{b)} \quad \lim_{t\to0} k_t = 0 \; , \\ &\text{c)} \quad \lim_{t\to0}\eta_t^2 k_t \neq 0 \quad \text{and} \quad \lim_{t\to0} k_t \neq 0 \; , \end{aligned}$$

we show that (24) holds on all the three cases.
In cases a) and b) it' straightforward to prove that the term in (22) goes to zero faster than (23) diverges. In the last case (c), thanks to hypothesis 2, the term in (23) goes to zero, independently on the other term, since the term (22) is an exponential with negative exponent $\forall\, x \in \mathbb{R}$ $\forall\, t > 0$, thus this term cannot diverge. Thus, the following holds

$$\lim_{t\to0}\nu_t(x) = 0 \quad \forall x \neq 0 \qquad\qquad \lim_{t\to0}\gamma_t = 0 \; .$$

We can now check whether the triplet satisfies the conditions in Sato (1999).

1. The triplet has no diffusion term.

2. ν_t is not decreasing wrt t.

3. $\nu_t(B)$ and γ_t are continuous, where $B \in \mathbb{B}(\mathbb{R}^+)$ and $B \subset \{x : |x| > \epsilon > 0\}$. The continuity for $t > 0$ is obvious, since it is a natural consequence of the composition of continuous functions. We have to prove that the limits of $\nu_t(B)$ and γ_t are 0. We have already proven that $\nu_t(x)$ is non decreasing in t and that $\lim_{t\to 0} \nu_t(x) = 0$, $\forall x \neq 0$. The convergence of $\nu_t(B)$ to 0 is due to the dominated convergence theorem.

□

The Lévy Bachelier model is the simplest case of the Additive process (21), that can be obtained choosing

$$\sigma_t = \hat{\sigma},\ \eta_t = \hat{\eta}\sqrt{t},\ k_t = \frac{\hat{k}}{t} \quad .$$

In this case, condition 1 of Lemma A.1 is satisfied because $p_t^{\pm}$ are constant in time, while p_t^* is decreasing, and condition 2 holds; thus the process is Additive. Moreover, the process is time-independent because the log-characteristic function (20) is linear in t.

The Additive Bachelier presented in this paper is another particular case of the Additive process (21) that, even being very parsimonious, i) presents the interesting analytical properties described in this study and ii) is able to obtain calibration results quite close to the more general (but not necessarily well posed) "Lévy fixed ttm" that has time dependent parameters that vary at each maturity. In this case, σ_t is s.t $\sigma_t^2 t$ is monotone (property naturally satisfied by the ATM vol in real markets) and

$$\eta_t = \eta,\ k_t = k \quad .$$

This observation allows us to prove Proposition 2.1, as shown in Appendix B.

Finally, let us observe that the Bachelier model corresponds to the limiting case of the Additive Bachelier for $k \to 0$.

Appendix B: Proofs

Before proving that the proposed process is Additive and martingale, let us mention an important property of the model, stated in the following Lemma.

Lemma B.1. (Equivalence in law of the process $\{f_t\}$)
The process $\{f_t\}_{t\geq 0}$ with characteristic function (2) *–for any given t– is equivalent in law to*

$$f_t \overset{law}{=} \sigma_t \sqrt{t}\, z \tag{25}$$

with

$$z := \eta\,(1 - G) - \sqrt{G}\, g \ , \tag{26}$$

where g is a standard normal rv and G a positive rv with Laplace exponent (3).

Proof. The Lemma can be proven observing that the left and the right side of equation (25) have the same characteristic function. The characteristic function of z

$$\ln \phi^{(z)}(u) := \ln \mathbb{E}\left[e^{i\,u\,z}\right] = \psi\left(i\,u\,\eta + \frac{u^2}{2};\ k,\ \alpha\right) + i\,u\,\eta \ \ ,$$

is s.t. it can be computed using iterated expectations (see, e.g., McNeil *et al.* 2015, Sect.3.2.2, p.77). □

Proof. **Proposition 2.1**
First, we demonstrate Additivity proving that the Additive Bachelier satisfies Lemma A.1. In this case, σ_t is s.t $\sigma_t^2 t$ is monotone and

$$\eta_t = \eta,\ k_t = k \quad .$$

Condition 1 of Lemma A.1 is satisfied because both $p_t^{\pm}$ and p_t^* are decreasing, while condition 2 holds.
Then, we demonstrate that the process is martingale using Lemma B.1 $\square$

Proof. **Proposition 2.2**
The proof reminds the one of Lewis (2001) for exponential Lévy processes. Let us define the Fourier transform and its inverse

$$\begin{cases} FT: \ \hat{\omega}(\xi) := \int_{-\infty}^{+\infty} \omega(z)\, e^{-i\xi z}\, \mathrm{d}z \\ IFT: \ \omega(z) := \dfrac{1}{2\pi} \int_{-\infty}^{+\infty} \hat{\omega}(\xi)\, e^{i\xi z}\, \mathrm{d}\xi \ , \end{cases}$$

the Parseval relation holds

$$\int_{-\infty}^{+\infty} p(z)\, \omega(z)\, \mathrm{d}z = \frac{1}{2\pi} \int_{-\infty}^{+\infty} \phi(\xi)\, \hat{\omega}(\xi)\, \mathrm{d}\xi \ .$$

where $p(z)$ is the pdf of z
Let $\chi \in \mathbb{R}$, the strike, and $z \in \mathbb{R}$ a rv with characteristic function $\phi(\xi)$ analytic for $\Im(\xi) \in (-p^-, p^+)$, the Fourier transform of the call option payoff $\omega(z) := [z-\chi]^+$. The two parts of the Fourier transform are:

$$\begin{aligned} \int_{-\infty}^{+\infty} e^{-i\xi z}\, \mathbb{1}_{\{z>\chi\}}\, \mathrm{d}z &= \frac{e^{-i\xi\chi}}{i\,\xi} && \Im(\xi) < 0 \\ \int_{-\infty}^{+\infty} z\, e^{-i\xi z}\, \mathbb{1}_{\{z>\chi\}}\, \mathrm{d}z &= \frac{e^{-i\xi\chi}}{-\xi^2} + \chi \frac{e^{-i\xi\chi}}{i\,\xi} && \Im(\xi) < 0 \ . \end{aligned}$$

Finally,

$$\mathbb{E}[z-\chi]^+ = \frac{1}{2\pi} \int_{-\infty}^{+\infty} \phi(\xi)\, \frac{e^{-i\xi\chi}}{-\xi^2}\, \mathrm{d}\xi \qquad \Im(\xi) < 0$$

where the integral path is considered slightly below the real axis.
Because the characteristic function $\phi(\xi)$ is analytic for $\Im(\xi) \in (-p^-, p^+)$, applying the Chauchy theorem, we obtain

$$\mathbb{E}[z-\chi]^+ = \frac{e^{-\chi\, a}}{2\pi} \int_{-\infty}^{+\infty} \phi\left(\xi - i\, a\right)\, \frac{e^{-i\xi\chi}}{\left(i\,\xi + a\right)^2}\, \mathrm{d}\xi$$

where $a \in (0, p^-)$. In the case we want to consider $a \in (-p^-, 0]$, we apply the residue theorem, as in Lee (2004b), Thm.5.1, 5.2.
For $a \in (-p^+, 0)$,

$$\mathbb{E}[z-\chi]^+ = -\chi + \frac{e^{-\chi\, a}}{2\pi} \int_{-\infty}^{+\infty} \phi\left(\xi - i\, a\right)\, \frac{e^{-i\xi\chi}}{\left(i\,\xi + a\right)^2}\, \mathrm{d}\xi \ ,$$

and for $a = 0$

$$\mathbb{E}[z-\chi]^+ = -\frac{\chi}{2} + \frac{e^{-\chi\, a}}{2\pi} \int_{-\infty}^{+\infty} \phi\left(\xi - i\, a\right)\, \frac{e^{-i\xi\chi}}{\left(i\,\xi + a\right)^2}\, \mathrm{d}\xi$$

$\square$

Proof. **Proposition 2.3**
The Proposition is a consequence of Lemma B.1 and a straightforward application of the iterated expectation. A call option is

$$C(x,t;\mathbf{p}) := B_0\,\mathbb{E}_0\,[F_t - K]^+ = B_0\,\mathbb{E}_0\,[f_t - x]^+ = B_0\,\sigma_t\,\sqrt{t}\,\mathbb{E}\,[z-y]^+ \;,$$

thus, using the law of iterated expectations

$$\mathbb{E}\,[\,\bullet\,] = \mathbb{E}[\mathbb{E}[\,\bullet\,|G]]$$

we get the first result.
The Bachelier option price can be obtained considering the rv G identically equal to 1, i.e. it corresponds to the case $k=0$. □

Proof. **Proposition 2.4** We can write the right hand side of equation (8) as

$$C_b\,(x,t;\mathscr{I}_t(x)) = B_0\,\sqrt{t}\,c_b\left(\frac{x}{\sqrt{t}},\mathscr{I}_t(x)\right) \;, \tag{27}$$

where c_b is a normalized Bachelier call price

$$c_b(y,\sigma) := -y\,\Phi\left(-\frac{y}{\sigma}\right) + \sigma\,\varphi\left(-\frac{y}{\sigma}\right) \;. \tag{28}$$

The following properties hold $\forall x \in \mathbb{R}$, for fixed maturity t:

(i) Vega is positive ;

(ii) $\mathbb{E}_0\,[F_t - K]^+ > [-x]^+$;

(iii) $\lim_{\sigma\to\infty} c_b\left(\frac{x}{\sqrt{t}},\sigma\right) = \infty$;

(iv) $\lim_{\sigma\to 0} c_b\left(\frac{x}{\sqrt{t}},\sigma\right) = \left[-\frac{x}{\sqrt{t}}\right]^+$.

The first property is a consequence of (19), the second is due to the Jensen inequality

$$\mathbb{E}_0\,[F_t - K]^+ > [\mathbb{E}_0[F_t - K]]^+ = [-x]^+$$

and the other two come from direct computation. The first property implies that $c_b(x/\sqrt{t},\sigma)$ is strictly increasing in σ, while the last three that it always exists a solution for (8), since the Bachelier call price C_b is obtained multiplying the normalized Bachelier call price c_b by a positive constant. Thus, $\forall x \in \mathbb{R}$ and $\forall t \in \mathbb{R}^+$, it exists a unique value for the Implied volatility $\mathscr{I}_t(x)$, solution of (8). □

Proof. **Proposition 2.5**
Thanks to the homogeneity property (in (18)) of the Bachelier formula applied to equations (4) and (7), the IV equation (8) becomes the (time independent) equation (11). Thus, its solution $I(y)$ does not depend on time. □

Proof. **Proposition 2.6**
We define the function $\mathscr{G}(y, I)$ as

$$\mathscr{G}(y,I) := c_b(y,I) - \mathbb{E}\left[c_b\left(y+\eta(G-1), \sqrt{G}\right)\right] \ .$$

The IV equation (11) is equivalent to

$$\mathscr{G}(y, I(y)) = 0 \ .$$

Thus, applying the implicit function Theorem (see, e.g., Rudin 1976), the function $I(y)$ is well-defined and $\mathscr{C}^1(\mathbb{R})$ if

$$\begin{cases} \mathscr{G}(y, I(y)) = 0 \\ \left.\dfrac{\partial}{\partial I}\mathscr{G}(y,I)\right|_{I=I(y)} \neq 0 \end{cases} \quad \forall y \in \mathbb{R} \ .$$

The first condition comes from the definition of $I(y)$ (the Bachelier formula is monotone in y, and the integral is well defined, so the equation for $I(y)$ is well defined).
For the second condition we recall the expression of the (normalized) Bachelier formula (5). Thus,

$$\frac{\partial}{\partial I}\mathscr{G}(y,I) = \frac{\partial}{\partial I}c_b(y,I) = \varphi\left(-\frac{y}{I}\right) > 0 \quad \forall y \in \mathbb{R} \ ,$$

where the last equality appears in Appendix A; this proves that $I(y) \in \mathscr{C}^1(\mathbb{R})$.
The derivative of $I(y)$ is given by

$$I'(y) = -\left.\frac{\partial_y \mathscr{G}(y,I)}{\partial_I \mathscr{G}(y,I)}\right|_{I=I(y)} \ ,$$

in this case

$$I'(y) = \frac{\Phi\left(-\frac{y}{I(y)}\right) - \mathbb{E}\left[\Phi\left(-\frac{y+\eta(G-1)}{\sqrt{G}}\right)\right]}{\varphi\left(-\frac{y}{I(y)}\right)} \ , \tag{29}$$

that is well defined since

$$\mathbb{P}\left(\Phi\left(-\frac{y+\eta(G-1)}{\sqrt{G}}\right) \in [0,1]\right) = 1 \ .$$

With some computations, we can prove that

$$I''(y) = \frac{\mathbb{E}\left[\frac{1}{\sqrt{G}}\varphi\left(\frac{y+\eta(G-1)}{\sqrt{G}}\right)\right]}{\varphi\left(-\frac{y}{I(y)}\right)} - \frac{1}{I(y)} + 2\frac{y}{I(y)^2}I'(y) \tag{30}$$

which is well defined $\forall y \in \mathbb{R}$, $\eta \in \mathbb{R}$, $k \in \mathbb{R}^+$. It is possible to compute the derivative of the Implied vol $I(y)$ at any order n via the following equation

$$\frac{d^n}{(dy)^n} c_b\left(y, I(y)\right) = (-1)^n \mathbb{E}\left[\frac{1}{\sqrt{G}}\, He\left(\frac{y+\eta(G-1)}{\sqrt{G}}, n-2\right)\varphi\left(\frac{y+\eta(G-1)}{\sqrt{G}}\right)\right]$$

where $He\left(\bullet, n\right)$ are the Hermite polynomials of order n □

Proof. **Proposition 2.7**
For a given y, we impose the IV equation (11), i.e.

$$c_b\left(y, I(y;\eta)\right) = \mathbb{E}\left[c_b\left(y+\eta\left(G-1\right), \sqrt{G}\right)\right] =: \mathscr{A}$$

where $\mathscr{A}$ is a positive value. We change $y \to (-y)$ and $\eta \to (-\eta)$ in both terms of the IV equation (11). The right hand side becomes

$$\mathbb{E}\left[c_b\left(-(y+\eta\left(G-1\right)), \sqrt{G}\right)\right] = y + \mathbb{E}\left[c_b\left(y+\eta\left(G-1\right), \sqrt{G}\right)\right] = y + \mathscr{A}$$

while the left hand side is

$$c_b\left(-y, I(-y;-\eta)\right) = y + c_b\left(y, I(-y;-\eta)\right) \ .$$

Thus, we have that

$$\begin{cases} c_b\left(y, I(y;\eta)\right) & = & \mathscr{A} \\ c_b\left(y, I(-y;-\eta)\right) & = & \mathscr{A} \ . \end{cases}$$

Because the value of Implied vol that solves both equations is unique, we have that

$$I(-y;-\eta) = I(y;\eta)$$

□

Proof. **Corollary 2.8**
The if condition is a consequence of Proposition 2.7

$$I(y;\eta=0) = I(-y;\eta=0) \ .$$

The only if is a consequence of Proposition 2.9. We can compute I_0', the ATM derivative of $I(y)$, that is an odd function of η, and it is equal to zero only if $\eta = 0$ □

Proof. **Proposition 2.9**
Thanks to Proposition 2.6, we can Taylor expand the Implied volatility $I(y)$ around the ATM

$$I(y) = I_0 + I_0'\, y + \frac{1}{2} I_0''\, y^2 + o(y^2) \, .$$

I_0 can be obtained from (11) observing that $c_b(0, I_0) = I_0/\sqrt{2\pi}$.
The implicit function Theorem implies that

$$I_0' = \left.\frac{\Phi\left(-\dfrac{y}{I(y)}\right) - \mathbb{E}\left[\Phi\left(-\dfrac{y+\eta(G-1)}{\sqrt{G}}\right)\right]}{\varphi\left(-\dfrac{y}{I(y)}\right)}\right|_{y=0} = \sqrt{2\,\pi}\left[\frac{1}{2} - \frac{1}{2}\left(1 + \mathbb{E}\left[\mathrm{erf}\left(\frac{\eta}{\sqrt{2}}\,\frac{1-G}{\sqrt{G}}\right)\right]\right)\right]$$

that is antisymmetric in η. The value of I_0'' can be obtained directly from the proof of Proposition 2.6 by (30) computed ATM

$$I_0'' = \left.\left(\frac{\mathbb{E}\left[\frac{1}{\sqrt{G}}\,\varphi\left(\frac{y+\eta(G-1)}{\sqrt{G}}\right)\right]}{\varphi\left(-\frac{y}{I(y)}\right)} - \frac{1}{I(y)} + 2\frac{y}{I(y)^2} I'(y)\right)\right|_{y=0} = \sqrt{2\pi}\,\mathbb{E}\left[\frac{1}{\sqrt{G}}\,\varphi\left(\eta\,\frac{1-G}{\sqrt{G}}\right)\right] - \frac{1}{I_0}$$

□

Proof. **Proposition 2.10** Because "the purely imaginary points on the boundary of the strip of regularity (...) are singular points of" the characteristic function (cf. Lukacs 1972, Th.3.1, p.12), to select the boundaries of the analyticity strip, we have to consider $u = ia$ with $a \in \mathbb{R}$, or equivalently for

$$- a\, \eta\, \sigma_t \sqrt{t} - \frac{a^2}{2} \sigma_t^2\, t > - \frac{(1-\alpha)}{k} \quad \Leftrightarrow \quad a \in (-p_t^-, p_t^+) \ ,$$

with

$$p_t^{\pm} = \frac{1}{\sigma_t \sqrt{t}} \left\{ \mp\eta + \sqrt{\eta^2 + 2\, \frac{(1-\alpha)}{k}} \right\} = \frac{1}{\sigma_t \sqrt{t}}\, p^{\pm} \ .$$

We apply Proposition 3.5 in Baviera and Massaria (2025) and obtain that

$$\lim_{x \to \pm\infty} \frac{\mathscr{I}_t(x)^2}{|x/\sqrt{t}|} = \frac{1}{p_t^{\mp} \sqrt{t}} \ ,$$

because the characteristic function of returns $\zeta_t := \frac{f_t}{\sqrt{t}}$ is $\phi_t\left(u/\sqrt{t}\right)$.
Finally, we observe that

$$\lim_{y \to \pm\infty} \frac{I(y)^2}{|y|} = \frac{1}{\sigma_t} \lim_{x \to \pm\infty} \frac{\mathscr{I}_t(x)^2}{|x/\sqrt{t}|} = \frac{1}{p^{\mp}}$$

□

Proof. **Proposition 3.1** It is a consequence of the homogeneity property (in (18)) of the Bachelier formula (4) applied to the IV equation (11). □

References

Abramowitz, M. and Stegun, I.A., 1948. *Handbook of mathematical functions with formulas, graphs, and mathematical tables*, vol. 55, US Government printing office.

Azzone, M. and Baviera, R., 2021. Synthetic forwards and cost of funding in the equity derivative market, *Finance Research Letters*, 41, 101841.

Azzone, M. and Baviera, R., 2023. A fast Monte Carlo scheme for additive processes and option pricing, *Computational Management Science*, 20 (1), 31.

Bachelier, L., 1900. Jeu de speculation (The theory of speculation), *Ph.D. dissertation*.

Barndorff-Nielsen, O.E., 1997. Normal inverse Gaussian distributions and stochastic volatility modelling, *Scandinavian Journal of statistics*, 24 (1), 1–13.

Baviera, R. and Massaria, M.D., 2025. Smile asymptotics for Bachelier Implied Volatility.

Black, F. and Scholes, M., 1973. The pricing of options and corporate liabilities, *Journal of Political Economy*, 81 (3), 637–654.

Brigo, D. and Morini, M., 2005. An empirically efficient analytical cascade calibration of the LIBOR Market Model based only on directly quoted swaptions data, *Available at SSRN 552581.*

Carr, P. and Torricelli, L., 2021. Additive logistic processes in option pricing, *Finance and Stochastics*, 25 (4), 689–724.

Carr, P. and Wu, L., 2003. The finite moment log stable process and option pricing, *The Journal of Finance*, 58 (2), 753–777.

CME, 2020. Switch to Bachelier options pricing model – Effective April 22, 2020, *Available at CME, www.cmegroup.com/content/cmegroup/en/notices/clearing/2020/04/Chadv20-171.html*, (20-171).

Cont, R. and Tankov, P., 2003. *Financial Modelling with jump processes*, Chapman and Hall/CRC.

Davis, M. and Etheridge, A., 2006. *Louis Bachelier's Theory of Speculation: the origins of modern finance*, Princeton University Press.

Gatheral, J., 2011. *The volatility surface: a practitioner's guide*, vol. 357, John Wiley & Sons.

ICE, 2020. Negative pricing and option model transition, *Available at ICE, www.theice.com/publicdocs/circulars/20057.pdf*, (20-057).

Lee, R.W., 2004a. The moment formula for implied volatility at extreme strikes, *Mathematical Finance*, 14 (3), 469–480.

Lee, R.W., 2004b. Option pricing by transform methods: extensions, unification and error control, *Journal of Computational Finance*, 7 (3), 51–86.

Lewis, A.L., 2001. A simple option formula for general jump-diffusion and other exponential Lévy processes, *Available at SSRN, 282110.*

Lukacs, E., 1972. A survey of the theory of characteristic functions, *Advances in Applied Probability*, 4 (1), 1–37.

Madan, D.B. and Seneta, E., 1990. The variance gamma (VG) model for share market returns, *Journal of business*, 511–524.

McNeil, A.J., Frey, R., and Embrechts, P., 2015. *Quantitative risk management: concepts, techniques and tools*, Princeton University press.

Medvedev, A. and Scaillet, O., 2006. Approximation and calibration of short-term implied volatilities under jump-diffusion stochastic volatility, *The Review of Financial Studies*, 20 (2), 427–459.

Rudin, W., 1976. *Principles of mathematical analysis*, 4.2, McGraw-Hill New York.

Sato, K.I., 1999. *Lévy processes and infinitely divisible distributions*, Cambridge University Press.

Shaikh, I., 2021. On the relation between the crude oil market and pandemic Covid-19, *European Journal of Management and Business Economics*, 30 (3), 331–356.

Notation and shorthands

Symbol	**Description**
$\mathbb{E}_s[\bullet]$	$\mathbb{E}_s[\bullet\vert\mathscr{F}_s]$ where $\mathscr{F}_s$ is the natural filtration
B_0	discount factor between the value date and option maturity t
F_s	Forward price with expiry in t and valued at time $s \in [0,t]$
$C_b\,(x,t;\sigma)$	Bachelier call option price wrt moneyness x and maturity t, with volatility σ
$c_b(y,\sigma)$	normalized Bachelier call option price wrt moneyness y, with volatility σ
$C\,(x,t;\mathbf{p})$	Additive Bachelier call price wrt moneyness x and maturity t, function of parameters $\mathbf{p}$
σ_t^{ATM}	ATM vol term structure observed on market data
$\sigma_t \in \mathbb{R}^+ \setminus 0$	vol term structure, a model parameter, a strictly positive continuous function
$\eta \in \mathbb{R}$	skew parameter
$k \in \mathbb{R}^+$	vol-of-vol parameter, a non-negative parameter
$\alpha \in [0,1)$	hyper-parameter of the model
$\mathscr{I}_t\,(x)$	Implied volatility wrt the moneyness x and the maturity t
$I\,(y)$	Implied volatility wrt the (normalized) *moneyness degree* y
$\mathcal{I}\,(\chi)$	Implied volatility wrt χ
G	a positive rv with unitary mean and variance k, Laplace transform $\psi(u;k,\alpha)$
$\Im(\xi)$	Imaginary part of a complex number ξ
$\phi_t\,(u)$	characteristic function of the underlying process $\{f_t\}_{t\geq 0}$, defined in equation (2)
$\varphi(\bullet), \Phi(\bullet)$	pdf and CDF of a standard normal rv
$\psi(u;k,\alpha)$	Laplace exponent of the positive rv G
$t_0 = 0$	value date
t	European option maturity (and time-to-maturity)
x	option moneyness, equal to $K - F_0$
y	$x/(\sigma_t\sqrt{t})$: (normalized) *moneyness degree*
χ	$x/(\sigma_t^{ATM}\sqrt{t})$: a normalized *moneyness*
ζ_t	$\frac{F_t - F_0}{\sqrt{t}}$: increment of forward price divided by the squared root of the time-to-maturity t
$\mathscr{C}^n(\mathbb{R})$	class of function n-times differentiable, with n-th derivative continuous

Symbol	Description
ATM	At-The-Money (referred to options)
bp	basis point (typical measurement unit for rates), equal to 0.01%
CDF	cumulative distribution function
CME	Chicago Mercantile Exchange
FT	Fourier transform
ICE	Intercontinental Exchange
iff	if and only if
IFT	inverse Fourier transform
ITM	In-The-Money (referred to options)
IV	Implied volatility
mkt	market
MSE	mean squared error
NIG	Normal Inverse Gaussian
OIS	Overnight Indexed Swap
OTM	Out-The-Money (referred to options)
pdf	probability density function
rv	random variable
ttm	time-to-maturity
VG	Variance Gamma
wrt	with respect to
WTI	West Texas Intermediate oil market